# Poster Contributions

https://doi.org/10.1017/S1743921318006695 Published online by Cambridge University Press

*Dwarf Galaxies: From the Deep Universe to the Present*
*Proceedings IAU Symposium No. 344, 2019*
*K. B. W. McQuinn & S. Stierwalt, eds.*

doi:10.1017/S1743921318006695

# The hydrodynamic evolution of the gas content in the dSph galaxy Ursa Minor induced by the feedback from types Ia and II supernovae

**Anderson Caproni[1], Gustavo A. Lanfranchi[1], Gabriel H. Campos Baião[1], Grzegorz Kowal[2] and Diego Falceta-Gonçalves[2]**

[1]Núcleo de Astrofísica Teórica, Universidade Cruzeiro do Sul,
R. Galvão Bueno 868, Liberdade, 01506-000, São Paulo, SP, Brazil
email: anderson.caproni@cruzeirodosul.edu.br

[2]Escola de Artes, Ciências e Humanidades, Universidade de São Paulo,
Rua Arlindo Bettio 1000, CEP 03828-000 São Paulo, Brazil

**Abstract.** Dwarf spheroidal galaxies of the Local Group share a similar characteristic nowadays: a low amount of gas in their interiors. In this work, we present results from a three-dimensional hydrodynamical simulation of the gas inside an object with similar characteristics of the Ursa Minor galaxy. We evolved the initial gas distribution over 3 Gyr, considering the effects of the types Ia and II supernovae. The instantaneous supernovae rates were derived from a chemical evolution model applied to spectroscopic data of the Ursa Minor galaxy. Our simulation shows that the amount of gas that is lost varies with time and galactocentric radius. The highest gas-loss rates occurred during the first 600 Myr of evolution. Our results also indicate that types Ia and II supernovae must be essential drivers of the gas loss in Ursa Minor galaxy (and probably in other similar dwarf galaxies).

**Keywords.** galaxies: dwarf — galaxies: evolution — galaxies: individual (Ursa Minor) — galaxies: ISM — hydrodynamics — methods: numerical

## 1. Introduction

Ursa Minor galaxy is located at a Galactocentric distance of ∼64 kpc (Irwin & Hatzidimitriou 1995). Similarly to other classical dSph galaxies, Ursa Minor is deficient in neutral gas (e.g., Mateo 1998, Grcevich & Putman 2009). External mechanisms, such as ram-pressure and tidal stripping are possible candidates behind the gas loss in dSph galaxies (e.g., Emerick *et al.* 2016), as well as, internal processes such as galactic winds triggered by supernovae (SNe) explosions (e.g., Ruiz *et al.* 2013, Caproni *et al.* 2015). In this work, we provide a brief overview of the first 3D-hydrodynamical simulations linked to observationally constrained chemical evolution model of the dSph galaxy Ursa Minor (see Caproni *et al.* 2017 for further details).

## 2. Methodology and results

We used the numerical code PLUTO (Mignone *et al.* 2007) to evolve the differential equations for the mass, momentum and energy quantities associated with an ideal gas under influence of a cored, static dark matter (DM) gravitational potential generated by an isothermal, spherically symmetric DM mass density profile (see Caproni *et al.* 2017 for further details).

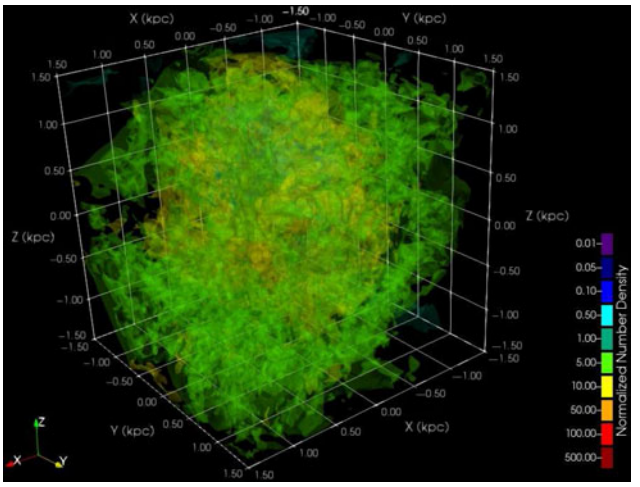


**Figure 1.** Spatial distribution of the number density (in units of 0.1 particles $cm^{-3}$) after 550 Myr of evolution. (A color version of this figure is available in the online proceedings.)

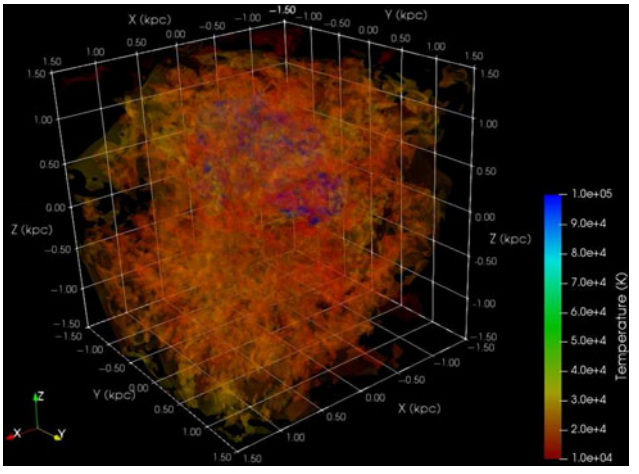


**Figure 2.** Spatial distribution of the temperature after 550 Myr of evolution. (A color version of this figure is available in the online proceedings.)

We adopted an initial gas density and pressure profiles obtained from hydrostatic equilibrium between an initial, isothermal gas and the DM gravitational potential induced by a total DM mass of $1.51 \times 10^9$ $M_\odot$. It produces centrally peaked distributions for the density and thermal pressure that decrease radially outward. The initial gas mass inside the tidal radius is approximately $2.94 \times 10^8$ $M_\odot$.

We simulated a cubic region of 3 kpc × 3 kpc × 3 kpc, using a grid with 256 points in each Cartesian direction (spatial resolution of 11.72 pc per computational cell). Types II and Ia SNe rates used in our simulation were derived by a chemical evolution model (CEM) that reproduces several observational constraints ([a/Fe], [Eu/Fe], [Ba/Fe] ratios, the present day gas mass, stellar metallicity distribution) of the dSph galaxy Ursa Minor (Lanfranchi & Matteucci 2004, Lanfranchi & Matteucci 2007). It is important to emphasize that the adopted CEM considers the stellar lifetimes in the calculations, a Kennicutt-Schmidt law prescription for the star formation (Schmidt 1963; Kennicutt 1998), and an initial stellar mass function of Salpeter (Salpeter 1955).

https://doi.org/10.1017/S1743921318006695 Published online by Cambridge University Press

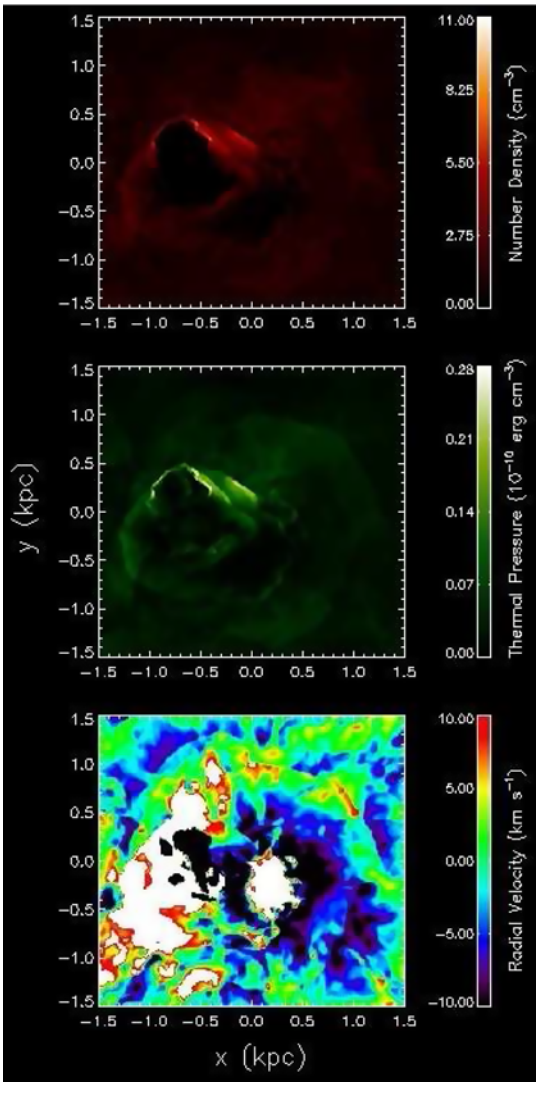


**Figure 3.** Spatial distribution of the number density (top panel), pressure (middle panel), and radial velocity (bottom panel) on $xy$ plane at $z = 0$ after 550 Myr of evolution. (A color version of this figure is available in the online proceedings.)

The imposed SN rates are strictly respected during the whole simulations, providing when a SN event must occur during hydrodynamical calculations. The SN sites are randomly chosen, with the denser regions more prone to be selected for a SN until 1.8 Gyr (epoch when type Ia SNe rate are roughly equal to type II SNe rate). After that, a totally random distribution of the SN sites are assumed in the simulation. This procedure constrains where a SN event must occur inside computational domain. Finally, an internal energy of $10^{51}$ erg is added into a spherical volume with a 2-cell radius and centered at the elected SN site (as in Caproni *et al.* 2015 and Caproni *et al.* 2017).

Under action of the SNe, the initial isothermal gas with a centrally peaked density profile becomes more sparse and morphologically distorted, as it is shown in Figs. (1) and (2). The multiple interactions of the SN remnants introduces turbulence into the interstellar medium (ISM), creating complex patterns in the gas distribution. Infall and outflow motions coexist inside galaxy, as it can be seen in Fig. (3). Galactic winds induced

https://doi.org/10.1017/S1743921318006695 Published online by Cambridge University Press

by SNe blasts are responsible for removing more than 60% of the initial gas mass inside the tidal radius of the galaxy, with the highest gas-loss rates occurring during the first 600 Myr of evolution. In other words, more than a half of the initial amount of gas is removed after 3 Gyr of evolution, reinforcing the importance of SNe feedback in such physical process.

## 3. Final remarks

Our main results can be summarized as follows: (1) Gas mass loss varies with time, as well as per galactic radius, in agreement with Caproni *et al.* (2015); (2) The more pronounced losses occurred approximately in the first 600 Myr for all galactic radii, in which type II SN rate adopted in this work reaches its maximum; (3) The central region of Ursa Minor ($r \leqslant 300$ pc) lost the largest amount of gas (∼90% of the initial mass) in the same interval; (4) After 3 Gyr of evolution, the remaining mass in gas for $r \leqslant 300$ pc is only ∼15% of its original value. For $r < 600$ pc, ∼24% of the initial mass still remains, increasing to ∼39% inside the tidal radius of Ursa Minor.

Those findings suggest that type II and Ia SNe explosions are the main mechanism behind the gas losses in Ursa Minor, even though additional external mechanisms, such as tidal and/or ram-pressure stripping, must have played a role in the gas loss history of Ursa Minor.

This work has made use of the computing facilities of the Laboratory of Astroinformatics (IAG/USP, NAT/UCS), whose purchase was made possible by the Brazilian agency FAPESP (grant 2009/54006-4) and the INCT-A. A.C. thanks the Brazilian agency CNPq (grant 305990/2015-2) and FAPESP (grants 2017/03173-4 and 2017/25651-5). The authors also acknowledge financial support from FAPESP through the grant 2014/11156-4.

## References

Caproni, A., Lanfranchi, G. A., Luiz da Silva, A. & Falceta-Gonçalves, D. 2015, *ApJ*, 805, 109
Caproni, A., Lanfranchi, G. A., Campos Baio, G. H., Kowal, G. & Falceta-Gonçalves, D. 2017, *ApJ*, 838, 99
Emerick, A., Mac Low, M., Grcevich, J., & Gatto, A. 2016, *ApJ*, 826, 148
Grcevich J., & Putman M. E., 2009, *ApJ*, 696, 385
Irwin, M., & Hatzidimitriou, D. 1995, *MNRAS*, 277, 1354
Kennicutt, R. C., Jr. 1998, *ApJ*, 498, 541
Lanfranchi, G. A., & Matteucci, F. 2004, *MNRAS*, 351, 1338
Lanfranchi, G. A., & Matteucci, F. 2007, *A&A*, 468, 927
Mateo, M. L. 1998, *ARA&A*, 36, 435
Mignone, A., Bodo, G., Massaglia, S., *et al.* 2007, *ApJS*, 170, 228
Ruiz, L. O., Falceta-Gonçalves, D., Lanfranchi, G.A., & Caproni, A. 2013, *MNRAS*, 429, 1437
Salpeter, E. E. 1955, *ApJ*, 121, 161
Schmidt, M. 1963, *ApJ*, 137, 758